ronic acid and type IV collagen were markedly elevated. The histological changes in the liver showed predominantly pericellular and perisinusoidal fibrosis with perivenular fibrosis. On immunohistochemical study, α-SMA-positive myofibroblast-like cells and CD42b-positive atypical cells in fibrotic or sinusoidal areas were seen.

Shiozawa *et al.*[2] performed a literature survey and found that 29 of 31 patients (93.5%) with TAM complicated by liver fibrosis in Down's syndrome died before the age of 150 days. Some patients with liver fibrosis were effectively treated with a brief course of low-dose cytarabine. Rapid reductions in blast numbers can contribute to clinical deterioration and early treatment may thus be beneficial. However, serum markers of liver fibrosis in our patient were already extremely high at birth. After treatment with cytarabine, WBC count and blast level were rapidly decreased. However, markers continued to increase and direct bilirubin was also elevated, suggesting the progression of liver fibrosis. Liver fibrosis can reach a critical state in TAM, and this can produce liver failure. Inchinkoto consists of spray-dried hot-water extracts of the following three medical herbs mixed: *Artemisia capillaris spica*, *Gardenia fructus* and *Rhei rhizome*. The drug has long been used in Japan and China as an anti-inflammatory, antipyretic, choleretic and diuretic agent for liver disorders and jaundice.[8] Inchinkoto has been reported to show potent inhibitory effects on the hepatocyte apoptosis induced by transforming growth factor β,[9] and it inhibits the production of inflammatory cytokines in concanavalin hepatitis.[10] In our patient, hyaluronic acid, type IV collagen, and direct bilirubin showed marked decreases after oral administration of inchinkoto. Inchinkoto may therefore have a therapeutic role in liver fibrosis with TAM. Our case report suggests that improvement of hepatic fibrosis predicts good outcome and that the Japanese herbal medicine inchinkoto is useful for treating hepatic fibrosis.

Acknowledgments

This work was partly supported by grants for MEXT KAKENHI (20591304). We wish to thank Dr Yoko Takeda, Dr Takashi Nakagawa and Dr Junka Haku for clinical support.

References

1 Lange B. The management of neoplastic disorders of haematopoiesis in children with Down's syndrome. *Br. J. Haematol.* 2000; **110**: 512–24.
2 Shiozawa Y, Fujita H, Fujimura J *et al.* A fetal case of transient abnormal myelopoiesis with severe liver failure in Down syndrome: Prognostic value of serum markers. *Pediatr. Hematol. Oncol.* 2004; **21**: 273–8.
3 Hoskote A, Chessells J, Pierce C. Transient abnormal myelopoiesis (TAM) causing multiple organ failure. *Intensive Care Med.* 2002; **28**: 758–62.
4 Tamura T, Kobayashi H, Yamataka A, Lane GJ, Koga H, Miyano T. Inchin-ko-to prevents medium-term liver fibrosis in postoperative biliary atresia patients. *Pediatr. Surg. Int.* 2007; **23**: 343–7.
5 Ahmed M, Sternberg A, Hall G *et al.* Natural history of GATA1 mutations in Down syndrome. *Blood* 2004; **103**: 2480–9.
6 Xu G, Nagano M, Kanezaki R *et al.* Frequent mutations in the *GATA-1* gene in the transient myeloproliferative disorder of Down syndrome. *Blood* 2003; **102**: 2960–8.
7 Miyauchi J, Ito Y, Kawano T, Tsunematsu Y, Shimizu K. Unusual diffuse liver fibrosis accompanying transient myeloproliferative disorder in Down's syndrome: A report of four autopsy cases and proposal of a hypothesis. *Blood* 1992; **80**: 1521–7.
8 Kiso Y, Ogasawara S, Hirota K *et al.* Antihepatotoxic Principles of Artemisia capillaris Buds1. *Planta Med.* 1984; **50**: 81–5.
9 Yamamoto M, Ogawa K, Morita M, Fukuda K, Komatsu Y. The herbal medicine Inchin-ko-to inhibits liver cell apoptosis induced by transforming growth factor beta 1. *Hepatology* 1996; **23**: 552–9.
10 Yamashiki M, Mase A, Arai I *et al.* Effects of the Japanese herbal medicine 'Inchinko-to' (TJ-135) on concanavalin A-induced hepatitis in mice. *Clin. Sci. (Lond)* 2000; **99**: 421–31.

LETTERS TO THE EDITOR

DOI: 10.1111/j.1939-165X.2011.00378.x

Successful immunostaining demonstrates abnormal intracytoplasmic *MYH9* protein (NMMHC-IIA) in neutrophils of a dog with May-Hegglin anomaly

We previously reported a case of May-Hegglin anomaly (MHA) in a dog.[1] During the investigation, immunostaining to demonstrate abnormal intracytoplasmic *MYH9* protein (non-muscle myosin heavy chain IIA, or NMMHC-IIA) in neutrophils was attempted, but was unsuccessful. Following publication, the corresponding author was contacted by Dr. Shinji Kunishima, who offered to perform immunostaining in his laboratory.

Blood smears from the dog with MHA had been prepared in 2007 and stored at -70°C. Upon removal from the freezer, blood smears were immediately wrapped tightly in plastic wrap to prevent formation of condensation on the sample and were thawed to room temperature. The control sample, submitted as part of the routine hematology caseload at the University of Tennessee Veterinary Medical Center Clinical Pathology Laboratory, was from a 9-year-old female spayed Cocker Spaniel with no significant hematologic abnormalities based on CBC and blood smear review. Fresh smears were made using EDTA-anticoagulated blood, were air-dried, and were neither fixed nor stained. Both sets of smears were shipped at room temperature to Dr. Kunishima and arrived at their destination within 3 days.

Peripheral blood smears were analyzed by immunofluorescence as described previously.[2] After blood smears were fixed in methanol and permeabilized with acetone, the cells were hydrated and blocked with normal goat serum. Slides were incubated with anti-human platelet NMMHC-IIA polyclonal antibody (BT561, Biomedical Technologies Inc., Stoughton, MA, USA) and reacted with Alexa Fluor 555-labeled goat anti-rabbit IgG. The cells were examined by fluorescence microscopy (BX50; Olympus, Tokyo, Japan).

Neutrophils from the control dog exhibited diffuse intracytoplasmic myosin IIA localization (Figure 1). In contrast, neutrophils from the dog with MHA contained atypical type I intracytoplasmic aggregation of myosin IIA (Figure 2) corresponding to the blue-gray cytoplasmic inclusions seen on Wright-stained smears by light microscopy.

In people, normal neutrophils exhibit diffuse, homogenous distribution of NMMHCA-IIA throughout the cytoplasm.[2,3] In people with *MYH9* disorders, 3 atypical localization patterns based on immunostaining have been described depending on the size and number of inclusions.[2] Type I localization (1-2 large, intensely stained, oval to spindle-shaped cytoplasmic foci against a weaker staining background) has been

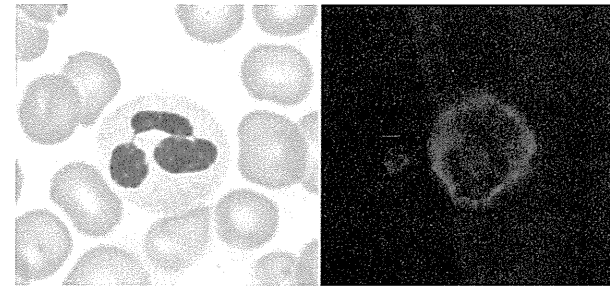

Figure 1. Blood smears from a control dog. x 100 objective. (**Left**) Normal neutrophil. Wright stain. (**Right**) Immunofluorescent micrograph of a neutrophil with diffuse localization of NMMHC-IIA in the cytoplasm. Alexa Fluor 555 dye.

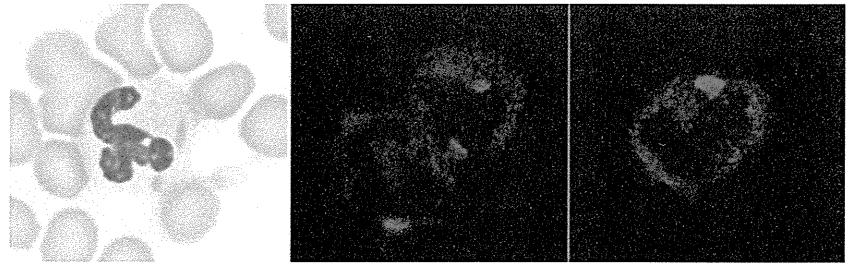

Figure 2. Blood smears from a dog with May-Hegglin anomaly. x 100 objective. (**Left**) Neutrophil with pale blue-gray, oval to fusiform inclusions. Wright stain. (**Center, Right**) Immunofluorescent micrographs of neutrophils with type I localization of NMMHC-IIA in the cytoplasm. Alexa Fluor 555 dye. (**Center**) Large, bright, elongate inclusions are found in neutrophils on the left (1 inclusion) and right (2 inclusions). (**Right**) Neutrophil with a large, bright, irregularly-shaped inclusion consistent with type I localization.

documented in people with MHA having an E1841K mutation[2] and is consistent with the pattern observed in our canine patient (also an E1841K mutation). It is thought that abnormal NMMHCA-IIA protein accumulates in the neutrophil cytoplasm, aggregating and interacting with ribosomes and microfilaments to create the inclusions.[2] In people, immunostaining may facilitate the diagnosis of *MYH9* disorders, given that faint staining of inclusions using Romanowsky-type stains (such as May-Grünwald Giemsa) has the potential to hamper diagnosis in some cases.[2,3] Additionally, immunostaining may reveal abnormal localization of intracytoplasmic myosin IIA, even when neutrophil inclusions are not detected by May-Grünwald Giemsa staining.[2]

In summary, we have demonstrated successful immunostaining of neutrophil inclusions from a dog with MHA using stored canine blood. Immunostaining of neutrophils using an anti-NMMHC-IIA antibody may be considered when evaluating macrothrombocytic thrombocytopenia of unknown origin, where *MYH9* mutation is a differential diagnosis.

Bente Flatland
Department of Biomedical and Diagnostic Sciences
College of Veterinary Medicine
University of Tennessee
bflatlan@utk.edu

Shinji Kunishima
Department of Advanced Diagnosis
Clinical Research Center, National Hospital Organization
Nagoya Medical Center
Nagoya, Japan
kunishis@nnh.hosp.go.jp

References

1. Flatland B, Fry MM, Baek SJ, et al. May-Hegglin anomaly in a dog. *Vet Clin Pathol.* 2011;40:207–214.
2. Kunishima S, Matsushita T, Kojima T, et al. Immunofluorescence analysis of neutrophil nonmuscle myosin heavy chain-A in MYH9 disorders: association of subcellular localization with MYH9 mutations. *Lab Invest.* 2003;83:115–122.
3. Kunishima S, Yoshinari M, Nishio H, et al. Haematological characteristics of MYH9 disorders due to MYH9 R702 mutations. *Eur J Haematol.* 2007;78: 220–226.

DOI: 10.1111/j.1939-165X.2011.00380.x

It's odd not to use odds

In the recent excellent article by Erb on pre-test probability, it was essential to insist on the importance of always taking pre-test probability into account when calculating/estimating predictive values and to make readers fully aware that most information published about predictive values without a clear indication of the pre-test probability is misleading.[1] Examples provided in this article are excellent illustrations of this point.

Unfortunately, many individuals, including clinicians, are reluctant to perform calculations, even using very simple 2 * 2 tables. I suggest that another approach may be used and is one that immediately demonstrates the importance of pre-test probability (Table 1). This approach involves: 1) calculation of odds, which is another way to formulate probabilities and is becoming more and more familiar in medicine, and 2) calculation of likelihood ratios (LR), which are a combination of sensitivity and specificity. These calculations indicate the prominent role of pre-test-probability, as post-test odds = pre-test odds * LR, and the calculations are easier to perform than 2 * 2 tables when multiple tests are used, as post-test odds = pre-test odds * LR_1 * LR_2 * and so on. These calculations can be approximated without a computer using simple arithmetic. There are also websites that offer freeware, such as Clinical Calculator 2 (faculty.vassar.edu/lowry/clin2.html) or nomograms (cebm.net/index.aspx?o=1043) to perform the calculations. The only

Table 1. Definition of terms.

Odds and Probabilities
If p = the probability of an event, odds of this event = p/(1-p). Example: if probability of disease X is 0.25 (25%), then odds of X are 0.25/0.75 = 0.33.
Knowing odds, probability p = odds / (1 + odds). Example: if odds of disease X = 0.33, then p = .33/(1 + 0.33) = 0.25 = 25%
Likelihood Ratios
Likelihood ratio of a positive result: LR+ = Se/(1-Sp), ie, the ratio of rates of true to false positive results
Likelihood ratio of a negative result: LR- = (1-Se)/Sp, ie, the ratio of rates of false to true negative results

Se indicates sensitivity; Sp, specificity.

CLINICAL REPORT

AMERICAN JOURNAL OF medical genetics PART A

Unusual Ribbon-Like Periventricular Heterotopia With Congenital Cataracts in a Japanese Girl

Rie Tsuburaya,[1] Mitsugu Uematsu,[1]* Atsuo Kikuchi,[1] Naomi Hino-Fukuyo,[1] Shinji Kunishima,[2] Mitsuhiro Kato,[3] Kazuhiro Haginoya[4] and Shigeru Tsuchiya[1]

[1]Department of Pediatrics, Tohoku University School of Medicine, Sendai, Japan

[2]Department of Advanced Diagnosis, Clinical Research Center, National Hospital Organization Nagoya Medical Center, Nagoya, Japan

[3]Department of Pediatrics, Yamagata University Faculty of Medicine, Yamagata, Japan

[4]Department of Pediatric Neurology, Takuto Rehabilitation Center for Children, Sendai, Japan

Received 3 November 2010; Accepted 27 June 2011

Periventricular heterotopia (PH), clumps of neurons mislocated beside the ventricle, is caused by failure to initiate migration during embryogenesis. We report on a 32-month-old Japanese girl with a unique subtype of PH, namely ribbon-like PH. The patient presented with severe psychomotor developmental delay, intractable epilepsy, and congenital cataracts and developed West syndrome phenotype. Brain magnetic resonance imaging revealed a unique undulating form of PH, categorized as ribbon-like PH, and other brain malformations including simplified gyri and dysgenesis of the corpus callosum. There was no evidence of prenatal TORCH infection or associated syndrome. Array-based comparative genomic hybridization revealed no chromosomal rearrangements. Genetic analyses of the *FLNA*, *DCX*, *ARX*, *LIS1*, and *TUBA1A* genes showed no mutations. Although little is known about ribbon-like PH, the clinical manifestations in our patient clearly differed from those in other reported patients.

Key words: ribbon-like periventricular heterotopia; migration disorders; congenital cataract; West syndrome

How to Cite this Article:
Tsuburaya R, Uematsu M, Kikuchi A, Hino-Fukuyo N, Kunishima S, Kato M, Haginoya K, Tsuchiya S. 2012. Unusual ribbon-like periventricular heterotopia with congenital cataracts in a Japanese girl.
Am J Med Genet Part A 158A:674–677.

INTRODUCTION

Heterotopia is one of the cortical malformations characterized by clumps of neurons in the wrong location of the brain. It is classified into three main groups by its location: periventricular, subcortical, and marginal glioneuronal heterotopia [Barkovich et al., 2005]. Periventricular heterotopia (PH) is diagnosed from the magnetic resonance imaging (MRI) finding of heterotopia lining the lateral ventricle. Most patients suffer from epilepsy and show variable developmental disability ranging from normal intelligence to severe mental retardation [Lu and Sheen, 2005]. Here, we report on a Japanese girl with a very rare form of PH called ribbon-like PH.

CLINICAL REPORT

A 32-month-old Japanese girl was born to healthy, nonconsanguineous parents at 40 weeks gestation. Her mother had no symptomatic infections and was negative on TORCH infection screening during pregnancy. She was the first child and had no family history of neurological disorders or inherited cataracts. Her birth height, weight, and head circumference were 48.0 cm (standard deviation [SD], +0.19), 3.2 kg (SD, +0.5), and 33.4 cm (SD, +0.07), respectively. The Apgar score 5 min after birth was 9. At 2 months of age, she was admitted to hospital with generalized tonic seizures that lasted for <1 min and occurred several times daily. She had short palpebral fissures and a faint pink patch on her forehead but no other facial dysmorphisms, such as a high forehead or the hypertelorism seen in Miller–Dieker syndrome (Fig. 1). She had normal female external genitalia and no anomalies of the extremities (Fig. 1). She showed poor head control, generalized muscle hypotonia, and no eye pursuit. She did not have feeding difficulty or respiratory failure.

Blood chemistry and metabolic analyses were normal. G-banding chromosome analysis from peripheral blood lymphocytes revealed a normal karyotype (46,XX). She had no deletions at chromosome 17p13.3 on fluorescence in situ hybridization using an LIS1 probe. Cardiac ultrasonography showed no abnormalities.

*Correspondence to:
Mitsugu Uematsu, Department of Pediatrics, Tohoku University School of Medicine, 1-1 Seiryo-machi, Aoba-ku, Sendai, Miyagi 980-8574, Japan.
E-mail: uematsu@bk.9.so-net.ne.jp
Published online 7 February 2012 in Wiley Online Library (wileyonlinelibrary.com).
DOI 10.1002/ajmg.a.34258

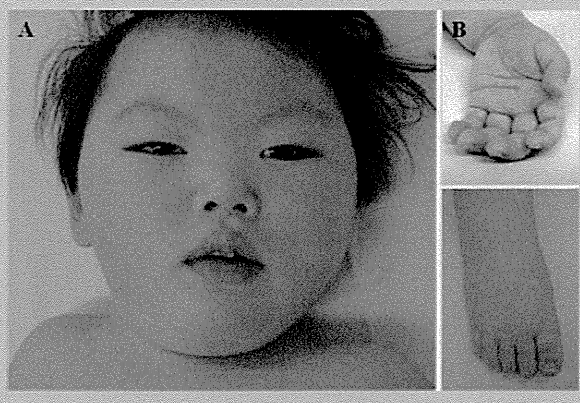

FIG. 1. The patient at 32 months of age. A: Note the short palpebral fissures and faint pink patch on the forehead. B: Note the normal extremities.

The ophthalmological examination revealed bilateral congenital cataracts without microphthalmia or abnormalities of the cornea and anterior chamber. The auditory brainstem response was within the normal range for her age. Electroencephalography (EEG) showed frequent spikes in the right temporal area during the interictal phase and spike bursts in the same area during the ictal phase.

Brain computed tomography showed symmetric enlarged ventricles and shallow sulci with no abnormal intracranial calcifications. Brain MRI showed diffuse simplified gyri with normal cortical thickness and enlarged lateral ventricles (Fig. 2). There was thin, symmetric laminar heterotopia encircling the lateral ventricles from the body to the posterior horns, with an undulating ribbon-like appearance. The corpus callosum showed an absent rostrum, tapered posterior, and absent splenium. The right cerebellar hemisphere was flattened by an arachnoid cyst and appeared as diffuse hypoplasia. Myelination was notably delayed for her age.

The seizures became resistant to multiple antiepileptic drugs, and her psychomotor development remained at the 2-month-infant level at 12 months of age. From 14 months of age, she developed a series of brief spasms and was diagnosed as West syndrome, with evidence of hypsarrhythmia on interictal EEG. With adrenocorticotropic hormone therapy, the spasms decreased to a few times a day, and the hypsarrhythmia disappeared on the EEG; however, frequent tonic seizures soon appeared. As the epilepsy proved to be difficult to control with multiple antiepileptic drugs, she had been maintained on ketogenic diet therapy since 18 months of age. As of now, at the age of 32 months, her physical growth has been normal, except the head circumference. The growth curves for height and weight are on the mean curve and on the −1 SD curve for Japanese girls, respectively. She has an acquired microcephaly at 44.5 cm (SD, −2.3). Her developmental quotient is 6.3, indicating arrested psychomotor development with no head control, eye pursuit, or meaningful words.

METHODS

All the examinations were performed after obtaining written informed consent and approval by the Institutional Review Board of Tohoku University Hospital. The patient's parents gave permission to publish of all the images, including the patient's pictures.

Mutation Analysis

Genomic DNA was extracted from peripheral blood using a SepaGene kit (Sanko Junyaku, Tokyo, Japan) according to the manufacturer's instructions. The mutation analyses of the *FLNA* (OMIM 30017), *DCX* (OMIM 300121), *ARX* (OMIM 300382), *LIS1* (OMIM 607432), and *TUBA1A* (OMIM 602529) genes were performed as described previously [Kato et al., 1999; Poirier et al., 2007; Kunishima et al., 2010]. The entire coding region of each gene was amplified by polymerase chain reaction (PCR). PCR amplicons were purified and subjected to direct cycle sequencing analyses using an automated sequencer.

Array-Based Comparative Genomic Hybridization

Array-based comparative genomic hybridization (array-CGH) was performed using the Agilent Human Genome Microarray kit 244A (Agilent Technologies, Santa Clara, CA) according to the manufacturer's instructions. The arrays were scanned with an Agilent scanner, processed using Agilent Feature Extraction software 9.5.3, and analyzed using Agilent Genomic Workbench Standard Edition 5.0.14.

Real-Time Automated PCR to Detect Cytomegalovirus DNA

For retrospective detection of congenital cytomegalovirus (CMV) infection, DNA was extracted from the preserved dried umbilical cord. Real-time automated PCR with the TaqMan method was performed as described previously [Machida et al., 2000].

RESULTS

The patient had no mutations in the five causative genes of the brain malformations: *FLNA*, *DCX*, *ARX*, *LIS1*, or *TUBA1A* genes. In the search for chromosomal rearrangements, array-CGH was analyzed and revealed no apparent deletions. CMV DNA was not detected from the dried umbilical cord.

DISCUSSION

In the development of the cerebral cortex during embryogenesis, there are three stages: neuronal proliferation and differentiation; migration toward the pial surface; and neuronal maturation and formation of six layers of cortex. PH is caused by failure to initiate migration, and neurons remain adjacent to the lateral ventricle [Guerrini and Parrini, 2010]. PH can be caused by extrinsic factors, such as irradiation and congenital infection, and can be associated with genetic syndromes, such as Ehlers–Danlos syndrome and various chromosomal abnormalities. The patient's mother had

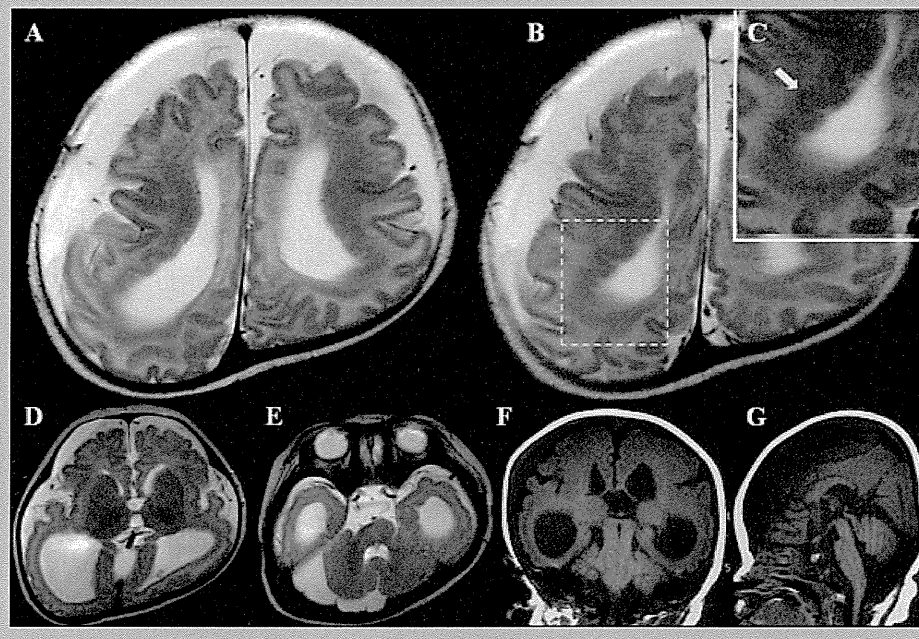

FIG. 2. Brain MRI at 3 months of age. Axial T2-weighted (3500/90, TR/TE) images (A–E) revealed diffuse simple gyri with normal cortical thickness, enlarged lateral ventricles, and diffuse cerebellar hypoplasia. Symmetric laminar heterotopia encircling the lateral ventricles from the body to the posterior horns had an undulating ribbon-like appearance (arrow in C, a higher power view of B). Coronal (F) and sagittal (G) T1-weighted (642/13, TR/TE) images revealed partial agenesis of the corpus callosum.

no evidence of TORCH infection. Additionally, we retrospectively ruled out prenatal CMV infection, which is often inapparent. Her clinical manifestations did not match any known genetic syndromes. The combination of multiple brain malformations and congenital cataract led us to perform array-CGH, which revealed no chromosomal rearrangements.

In some neuronal migration disorders, correlations between genotypes and phenotypes have been established [Kato and Dobyns, 2003]. Although the clinical manifestations and brain malformation of our patient differed from the classic phenotypes for each gene, we sequenced the *FLNA*, *DCX*, *ARX*, *LIS1*, and *TUBA1A* genes and found no mutations. None of the genes causing congenital cataracts are known to be related to brain malformations [Hejtmancik, 2008].

Based on the clinical records and MRI findings of 182 patients with PH, Parrini et al. [2006] classified PH into 15 phenotypic

TABLE I. The Clinical Manifestations of Three Patients With Ribbon-Like PH

	Our patient	Two reported patients
Sex	Female	1 male and 1 female
Age	32-month-old	Early adulthood
Age at onset	2-month-old	Childhood
Symptoms at onset	Seizures	Seizures
Intelligence	Severe mental retardation	Normal intelligence
Distribution of heterotopia around LV	Body to posterior	Posterior
Associated brain abnormalities	Simplified gyri, corpus callosum dysgenesis, cerebellar hypoplasia, delayed myelination	None
Inheritance	Sporadic	Sporadic
Mutational analysis	*FLNA*, *DCX*, *ARX*, *LIS1*, *TUBA1A*: no mutations	*DCX*: no mutations in one patient

LV, lateral ventricles.

subclasses by shape, location, and associated malformations or syndromes. Among the 182 patients, two unrelated patients were categorized as laminar-shaped, posterior ribbon-like PH, which was described that the heterotopic ribbon appeared convoluted with a nearly sinusoidal regularity. Our patient can be included in ribbon-like PH, but her phenotype was clearly different from that of two reported patients (Table I). Both of the reported patients manifested childhood-onset epilepsy but had no psychomotor disabilities and no other brain malformations or complications. In our patient, the PH was spread widely from the body to the posterior horns of the lateral ventricles, whereas the PH in the reported patients was limited to the posterior area. A mutational analysis of the *DCX* gene performed in one patient found no mutations. The pathomechanism of this unique ribbon-like form has not been elucidated.

In conclusion we report on the first detailed analysis of ribbon-like PH patient with the associated brain malformations, congenital cataracts, and West syndrome. Little is known of the genetic background of PH, including ribbon-like PH. Additional case reports and further genetic analyses should provide new insights into its pathogenesis.

REFERENCES

Barkovich AJ, Kuzniecky RI, Jackson GD, Guerrini R, Dobyns WB. 2005. A developmental and genetic classification for malformations of cortical development. Neurology 65:1873–1887.

Guerrini R, Parrini E. 2010. Neuronal migration disorders. Neurobiol Dis 38:154–166.

Hejtmancik JF. 2008. Congenital cataracts and their molecular genetics. Semin Cell Dev Biol 19:134–149.

Kato M, Dobyns WB. 2003. Lissencephaly and the molecular basis of neuronal migration. Hum Mol Genet 12:R86–R96.

Kato M, Kimura T, Lin C, Ito A, Kodama S, Morikawa T, Soga T, Hayasaka K. 1999. A novel mutation of the doublecortin gene in Japanese patients with X-linked lissencephaly and subcortical band heterotopia. Hum Genet 104:341–344.

Kunishima S, Ito-Yamamura Y, Hayakawa A, Yamamoto T, Saito H. 2010. FLNA p.V528M substitution is neither associated with bilateral periventricular nodular heterotopias nor with macrothrombocytopenia. J Hum Genet 55:844–846.

Lu J, Sheen V. 2005. Periventricular heterotopia. Epilepsy Behav 7:143–149.

Machida U, Kami M, Fukui T, Kazuyama Y, Kinoshita M, Tanaka Y, Kanda Y, Ogawa S, Honda H, Chiba S, Mitani K, Muto Y, Osumi K, Kimura S, Hirai H. 2000. Real-time automated PCR for early diagnosis and monitoring of cytomegalovirus infection after bone marrow transplantation. J Clin Microbiol 38:2536–2542.

Parrini E, Ramazzotti A, Dobyns WB, Mei D, Moro F, Veggiotti P, Marini C, Brilstra EH, Dalla Bernardina B, Goodwin L, Bodell A, Jones MC, Nangeroni M, Palmeri S, Said E, Sander JW, Striano P, Takahashi Y, Van Maldergem L, Leonardi G, Wright M, Walsh CA, Guerrini R. 2006. Periventricular heterotopia: Phenotypic heterogeneity and correlation with Filamin A mutations. Brain 129:1892–1906.

Poirier K, Keays DA, Francis F, Saillour Y, Bahi N, Manouvrier S, Fallet-Bianco C, Pasquier L, Toutain A, Tuy FP, Bienvenu T, Joriot S, Odent S, Ville D, Desguerre I, Goldenberg A, Moutard ML, Fryns JP, van Esch H, Harvey RJ, Siebold C, Flint J, Beldjord C, Chelly J. 2007. Large spectrum of lissencephaly and pachygyria phenotypes resulting from *de novo* missense mutations in tubulin alpha 1A (TUBA1A). Hum Mutat 28:1055–1064.